Space PV Concentrators for Outer Planet and Near-Sun Missions, Using Ultra-Light Fresnel Lenses Made with Vanishing Tools

Mark O'Neill[1], A.J. McDanal[1], Geoffrey Landis[2], Robert Pricone[3], Challa Kumar[4], Megan Puglia[4]

[1]Mark O'Neill, LLC, Keller, TX 76248,

[2]NASA Glenn Research Center, Cleveland, OH 44135,

[3]10X Technology LLC, Libertyville, IL 60048,

[4]University of Connecticut, Storrs, CT 06269

***Abstract* — Working under a NASA-funded Small Business Innovation Research (SBIR) program, our team has made additional progress in the development of space photovoltaic concentrators for outer planet and near-sun missions. One noteworthy innovation is in the scalable method of producing the ultra-light Fresnel lenses which provide the optical concentration of sunlight for both point-focus and line-focus concentrators. The new method uses "vanishing" lens molding tools. The paper will present the latest advances in this technology.**

***Index Terms* — concentrator, Fresnel lens, multi-junction cells, ultralight, graphene.**

I. Introduction and Summary

As discussed in previous papers [1]-[4], we have been working for the past several years on advanced space photovoltaic concentrator technology using three key elements:

1. Ultralight, robust, color-mixing, flat Fresnel lens optical elements. The latest lenses are strengthened with either:
   - A ceria-doped glass superstrate to support the silicone prisms forming the lens, or
   - An embedded mesh in the silicone lens itself.

2. Advanced multi-junction solar cells of two types:
   - 3-junction germanium based solar cells, or
   - Inverted metamorphic multi-junction (IMM) solar cells with at least 4 junctions to enhance conversion efficiency.

3. Waste heat radiators made from graphene, a material with unprecedented in-plane thermal conductivity. The latest radiators also have new features:
   - The graphene is deposited onto the back side of a reflective aluminum foil using innovative methods, and
   - The bi-material radiator can mitigate both low-intensity, low-temperature (LILT) effects and high-intensity, high-temperature (HIHT) effects for deep space and near-sun missions, respectively.

We have developed both 4X line-focus concentrators requiring only single-axis sun-tracking (with radiator/solar cell articulation for large longitudinal incidence angles) and 25X point-focus concentrators requiring two-axis sun-tracking. This paper will present technology advances in the past year for both types of concentrators, particularly in the manufacture of the Fresnel lenses (line-focus and point-focus).

The current work has focused on developing production techniques to bring the technology to flight readiness and on enhancing and verifying the mechanical robustness of the refractive concentrators.

II. Description of the Concentrator Modules

Fig. 1 shows both the line-focus and point-focus concentrator modules, including the lens, photovoltaic cell assembly, and graphene-based radiator. Note that the two concentrator modules share many important features. The nominal 4X and 25X geometric concentration ratios (lens aperture area / cell active area) correspond to sun-pointing error tolerances of ± 2° about the critical axis for line-focus and about both axes for point-focus. LILT mitigation is accomplished by the optical concentration itself, as discussed by Landis *et al.* [5]-[6].

For the 4X line-focus concentrator, the cell irradiance at the focal plane remains about 1 AM0 sun out to 2 AU distance from the sun, where the incident solar irradiance is 1/4th of 1 AM0 sun. For the 25X point-focus concentrator, the cell irradiance remains about 1 AM0 sun out to 5 AU distance from the sun, where the incident solar irradiance is 1/25th of 1 AM0 sun.

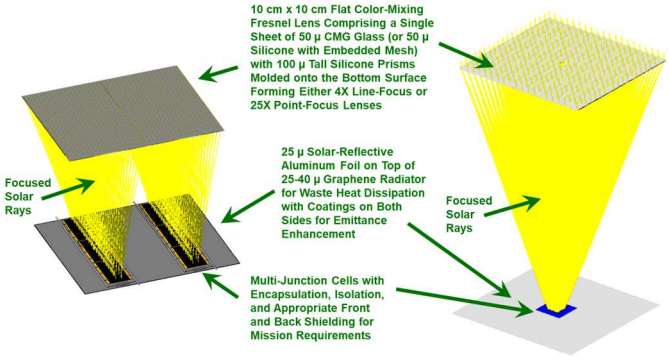

Fig. 1. 4X Line-Focus and 25X Point-Focus PV Concentrators Share Many Common Features.

Even deep space missions often use a near-sun inner planet swing-by as a gravity assist maneuver to reduce the propellant needed to reach an outer planet, exposing the cells to both HIHT and LILT effects over the course of the mission. Mitigation of high temperatures in the high solar intensity (near sun) environments can be accomplished by intentionally defocusing the lens by shortening (or lengthening) the spacing between the lens and solar cell, allowing part of the focused sunlight to miss the cell and instead intercept the reflective aluminum foil surrounding the cell. By reflecting away part of the sunlight, the irradiance on the cell can be maintained near 1 AM0 sun at < 1 AU distance from the sun, thereby keeping the cell at a mild operating temperature, and thus allowing the same concentrator assembly to be used for both the near-sun and the outer solar system power.

For a Venus swing-by, since Venus is about 0.7 astronomical units (AU) from the sun compared to Earth at 1.0 AU, the solar irradiance is about twice as high near Venus compared to near Earth. Reflecting half the focused sunlight away will therefore keep the cell temperature and the power output at approximately the same value as at 1 AU with the cell in its normal position relative to the lens. This concentrator technology will be deployed and supported as a dual (lens blanket and radiator blanket) flexible-blanket array, and the HIHT mitigation will be accomplished by moving the two blankets slightly closer together at array to sun distances less than 1 AU.

The low-temperature of the LILT environment is of lesser importance than the low intensity. Low temperatures are somewhat mitigated by the presence of the lens in front of the radiator, providing a thermal radiation barrier, which slightly increases the radiator and cell operating temperature. If desired, the temperature can be further mitigated by allowing the bi-material radiator to curl up due to differential thermal contraction, reducing the radiator view factor to deep space and keeping the cell temperature a little bit warmer still. The combined effect of the lens and "nyctinastic" radiator can be to keep the cell about 20 °C warmer near Jupiter (about 5 AU from the sun) than a one-sun cell under the same conditions.

III. Recent Lens Developments

As discussed in previous papers [1]-[4], our lenses use a unique color-mixing approach wherein neighboring prisms in the Fresnel lens have their angles slightly tweaked to intentionally overlap various portions of the solar spectrum to produce a similar current concentration profile over the cell for each of the various junctions in the cell, thereby avoiding "chromatic aberration" power losses in monolithic multi-junction solar cells.

Early versions of the planar concentrator lens were tested using only silicone for the Fresnel lens material, with no mechanical substrate or reinforcement. While these lenses had sufficient strength in ground testing, space testing showed that the lenses embrittled in the UV/radiation environment, leading to tearing of the lens [7]. Thus, the current version of the Fresnel lenses incorporates additional mechanical strength [1]. For improved mechanical robustness of our lenses, we have recently developed two new styles of robust lenses which use different strengthening elements for the relatively weak silicone lens material:

1. A ceria-doped glass superstrate lens using 50 to 100-micron CMG glass from Qioptiq to support the 100-micron-tall silicone prisms on the inside surface of the lens

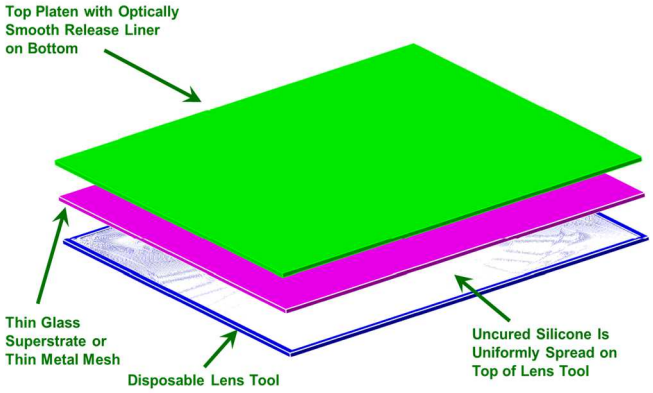

Fig. 2. Ultra-Light Fresnel Lens Manufacturing Approach.

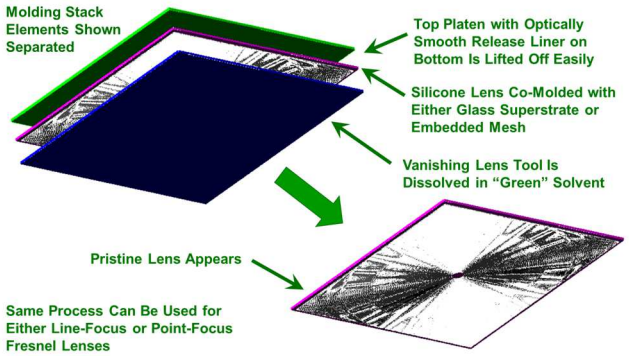

Fig. 3. "Vanishing" Lens Molding Tool Approach.

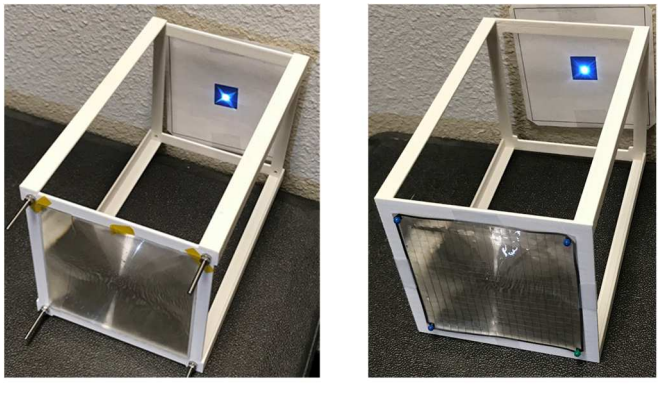

Fig. 4. Prototype Lenses Made with "Vanishing" Lens Molding Tools, Showing the Focal Spot.

2. New high-transmissivity embedded meshes to support the 100-micron silicone lens, including 50-micron photo-etched titanium mesh.

For scalable mass-production of these two new styles of robust lenses, we have developed a molding process using disposable polymer lens molding tools, as described in Fig. 2. The only difficult step in the manufacturing process is the removal of the molding tool from the cured silicone lens assembly at the end of the process. To overcome this difficult step, we have recently developed a novel approach which eliminates this tool removal step. Instead of removing the tool, we dissolve the tool in a "green" solvent, exposing the final lens assembly. This eliminates damage to the lens assembly due to mechanical removal of the lens tool. Fig. 3 shows this novel process.

Recently, we have proven the technical feasibility of the novel process by making lenses of both styles, as shown in Fig. 4.

We have had success with several different pairs of "vanishing" lens molding tool materials and appropriate green solvents, including:

1. Polystyrene (PS) molding tools and limonene solvent
2. Polymethyl methacrylate (PMMA) molding tools and anisole solvent.

Molding tools of both polymer materials were made by 10X Technology using nickel electroform replicas of the master diamond-turned tool. Fig. 5 shows one of the electroforms and Fig. 6 shows one of the polymer molding tools.

Fig. 5. Nickel Electroform Replica of Master Tool.

We have developed a simple, scalable process to dissolve the polymer molding tool quickly and efficiently using a green solvent for both styles of robust lenses. Fig. 7 shows two lenses made by using PMMA tools to mold 100-micron tall silicone prisms onto 100-micron thick ceria-doped glass superstrates in the anisole solvent bath during the molding tool dissolving process. We found that ultrasonic vibration of the solvent accelerates the dissolving process. We also found that a mesh basket provides easy handling of the thin lenses to avoid cracking the thin glass superstrates.

Fig. 6. Polymer Molding Tool Made from Electroform.

Fig. 7. Two Glass Superstrate Lenses in Ultrasonic Solvent Bath.

Fig. 8 shows one of the glass superstrate lenses after the polymer molding tool was dissolved. The process is simple and rapid, taking only a few minutes to dissolve the tool.

Fig. 9 shows two lenses made by using PMMA tools to mold silicone lenses with 100-micron tall silicone prisms and a 50-micron base layer with a 50-micron thick titanium mesh embedded in the base layer in the anisole solvent bath during the molding tool dissolving process. We learned that the unsupported lenses tended to curl up during the dissolving process due to absorption of the solvent by the silicone. We then used simple fixtures to pin the four corners of the mesh during the dissolving process to minimize this curling effect.

Fig. 10 shows one of the embedded mesh lenses after the polymer molding tool was dissolved. The process is simple and rapid, taking only a few minutes to dissolve the tool.

We made several of each type of lens (glass superstrate and embedded mesh) with 100% yield and no significant problems

Fig. 8. Glass Superstrate Lens After Dissolving Tool.

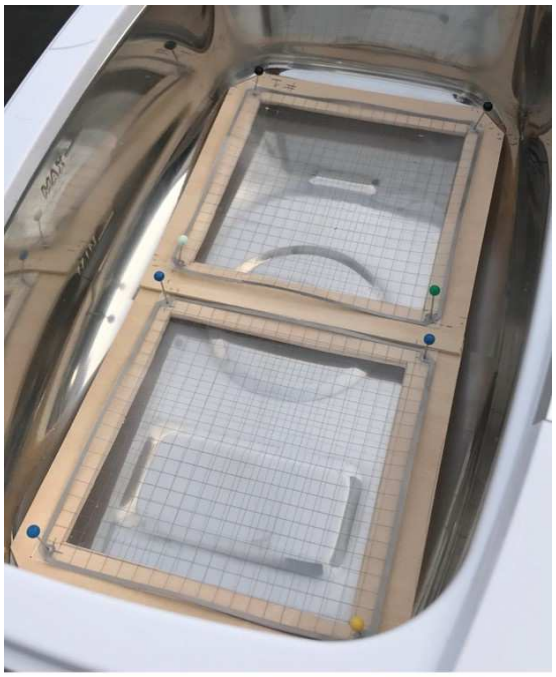

Fig. 9. Two Silicone Lenses with Embedded Titanium Mesh in Ultrasonic Solvent Bath.

to validate the "vanishing lens tool" process. The latest mesh-supported lenses are the lightest lenses we have ever made, with a typical mass of about 1.1 gram for a lens aperture area of 10 cm x 10 cm = 100 cm^2.

As described in previous papers [1]-[4], the embedded mesh lenses typically have about 85% optical efficiency compared to about 90% optical efficiency for the glass superstrate lenses, due to approximately 5% light blockage by the mesh. If such a 100 cm^2 mesh lens is used to focus sunlight onto a 30% efficient multi-junction solar cell, the power output of the lens/cell combination would be about 3.44 Watts for an earth-orbiting spacecraft (1 AM0 sun irradiance on lens). Thus, the mass/power parameter for the lens is only 0.32 g/W = 0.32 kg/kW. This ratio is often called the "alpha" parameter in the literature and is extremely important for most space missions. The alpha parameter of the lens of course needs to be

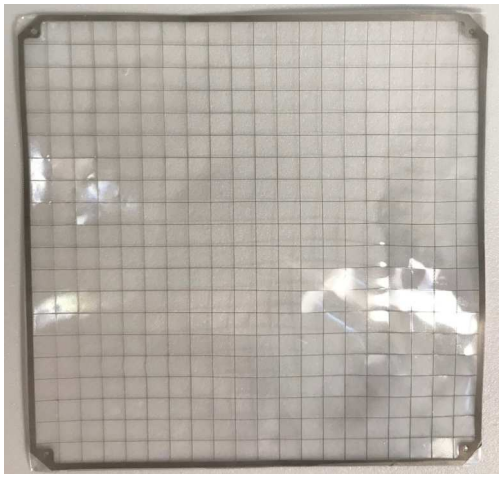

Fig. 10. Embedded Mesh Lens After Dissolving Tool.

added to the alpha parameters for the solar cell package, the waste heat radiator, the array deployment and support structure, etc., to fully quantify the mass/power ratio of the solar array system.

Since the lens also increases the irradiance onto the solar cell by a net factor of about 21X (85% lens transmittance times 25X geometric concentration ratio), it also dramatically reduces the alpha parameter of the solar cell package compared to conventional one-sun solar cell arrays.

IV. Recent Graphene Radiator Developments

For high concentration ratios, efficiency is increased under operational conditions by conducting the waste heat away from the active cell area and radiating it to space from both the front and back sides of the concentrator assembly (Fig. 1). In our system, this is achieved by use of graphene, which has an exceptionally high (in-plane) thermal conductivity [2]-[4]. Under a recent NASA STTR contract, our team worked with the University of Connecticut to develop novel methods of making and depositing bio-graphene onto aluminum foil to function as a bi-material thermal conductor to spread heat across the radiator surface. This novel method of making and depositing graphene allows tapering of the graphene thickness to optimize the heat spreading over the radiator area. Fig. 11 is

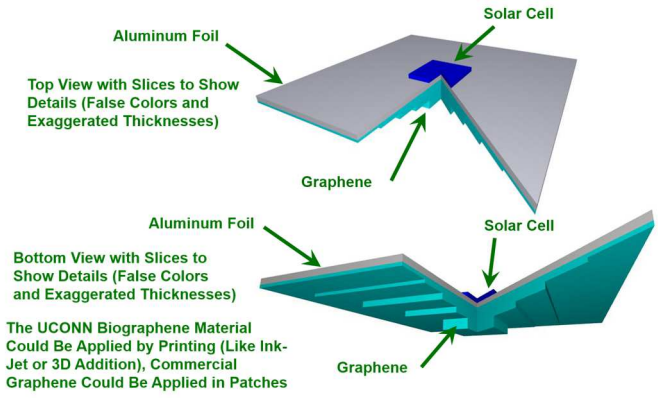

Fig. 11. Crude Schematic of Graphene Tapering Concept.

a schematic of the basic concept, with thicknesses exaggerated and false colors.

We have recently conducted thermal analyses that show a major reduction in cell operating temperature is achieved by tapering the graphene thickness rather than keeping the graphene thickness constant over the radiator. For the same total mass of graphene, the peak radiator temperature on GEO for the point-focus concentrator can be significantly reduced by tapering the graphene thickness, as shown in Fig. 12.

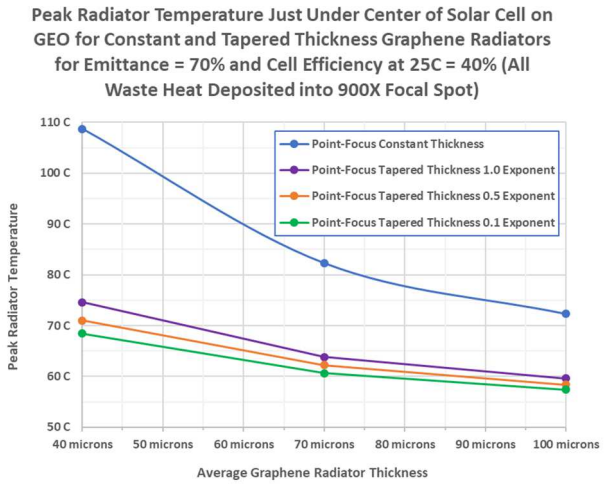

Fig. 12. Thermal Performance of Tapered Versus Constant Thickness Graphene Radiators on GEO.

For this analysis, the thickness of the graphene is varied from a maximum value at the center of the radiator to a zero value at the four adiabatic edges of the radiator. We varied the tapering curve from linear (1.0 exponent in Fig. 12) to non-linear (other exponents in Fig. 12). Note that for a 40-micron average thickness, the peak temperature is about 35-40ºC lower with tapering than without tapering, a substantial reduction with no mass penalty. For larger average graphene thicknesses, the peak temperature reduction is smaller, but still worthwhile.

For this analysis, we assumed the use of an emittance-enhancing coating on the graphene and aluminum foil, both of which have relatively low emittances in their uncoated form. Our team has recently tested a simple 25-micron coating of silicone on the graphene, which increased the emittance from 33% to 70% in testing by the Air Force Research Lab in Albuquerque. The total mass of a 10 cm x 10 cm silicone-coated radiator using 25-micron aluminum foil and 40-micron average thickness graphene is only 2.1 grams. Therefore, the alpha parameter for the bi-material radiator based on the 3.44 Watts of cell power output discussed in the previous section is only 0.61 g/W = 0.61 kg/kW.

Another advantage of the tapered graphene thickness is the greater radiation shielding of the solar cell from charged particles (electrons and protons) incident on the back side of the array. The greater thickness of graphene under the cell desired for improved lateral thermal conduction also provides reduced radiation degradation of the solar cell and improved end of life power. For all the tapered graphene thicknesses in Fig. 12, regardless of the taper exponent, the graphene is over 100 microns thick behind the entire solar cell. Together with the 25-micron aluminum foil and the 25-micron silicone coating, these materials provide over 125 microns of equivalent fused silica shielding for the back of the cell. The cell superstrate or carrier and the adhesive between the cell package and the radiator add to this equivalent fused silica shielding thickness for the solar cell.

If the multi-junction solar cell is an inverted metamorphic (IMM) type of cell, the cell package mass will be dominated by the front and back shielding. As discussed above, the tapered graphene radiator provides over 125 microns of equivalent fused silica shielding for the back of the cell. If an equivalent 125 microns of fused silica shielding is also used on the front of the cell, this will add approximately 0.13 grams of front shielding mass to the 2 cm x 2 cm solar cell. The alpha parameter, based on the previously discussed 3.44 Watts of cell power, for this front shielding is only 0.04 g/W = 0.04 kg/kW.

V. Performance Metrics and Cost Savings

Based on the mass discussions in the previous two sections, the combined alpha parameter for the mesh lens, the tapered graphene radiator, and the front cell shielding is 0.97 kg/kW. While this parameter is calculated from just the mass of these three elements (not including the array deployment and support structure, the harnessing, *etc*.), it is still important for comparison to the shielded one-sun solar cell used in a conventional solar array.

The inverse of this parameter is the specific power. For just the combined lens, radiator, and cell shielding, the specific power is about 1,035 W/kg. If the same 2 cm x 2 cm cell with the same front and back shielding was used at one sun irradiance, it would produce about 0.16 W (assuming 30% efficiency in earth orbit at 1 AMO sun irradiance). The front and back shielding would have a mass of 0.13 g (front) + 0.13 g (back) = 0.26 g (total), as discussed above. Thus, the alpha parameter for one-sun shielding would about 1.53 g/W = 1.53 kg/kW. The specific power for the one-sun cell shielding alone would be about 656 W/kg, less than two-thirds that of the 25X concentrator lens, radiator, and cell shielding.

For many missions, however, long lifetime in a high-radiation environment is a design objective, and thicker radiation shielding is required. As shown in Fig. 13, as the thickness of the cell radiation shielding increases, the advantage of the concentrator grows rapidly, due to the much higher power output of the cell under concentration. Radiation shielding at low mass penalty is one of the hallmark attributes of concentrator technology.

This attribute is of particular importance for future NASA missions. Missions are being proposed to orbit or even land on the inner moons of Jupiter, for example, but this requires operation in an environment with low solar intensity, low operating temperature, and a high radiation intensity. For this application the ability to incorporate thick radiation shield on

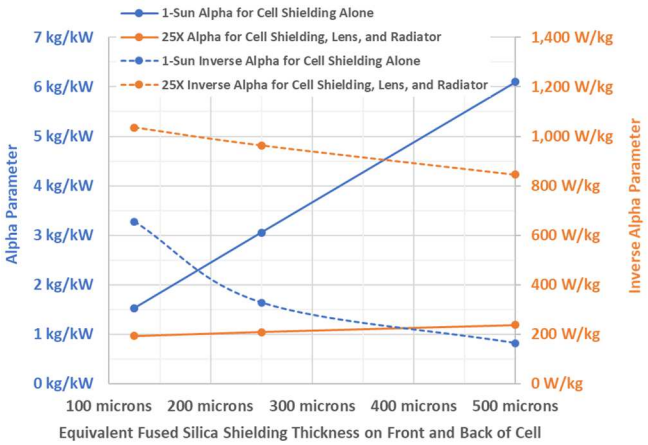

Fig. 13. Alpha, in kg/kW, and Specific Power (Inverse Alpha) Parameters for Key Elements of 25X Concentrator vs. One-Sun Cells.

the cells with only modest mass increase can be an enabling technology [5].

Our team has worked closely with larger firms to incorporate the Fresnel lens photovoltaic concentrators into state-of-the-art deployment and support platforms. One recent NASA-funded program performed by Orbital-ATK (now Northrop Grumman) looked in detail at the performance metrics and cost savings of the 25X point-focus concentrator on the compact telescoping array (CTA) [8]. Fig. 14 shows the basic solar array approach. The results were very positive, as summarized in Fig. 15.

Note in Fig. 15 that the cost savings and mass savings are more than 50% for the concentrator array compared to one-sun arrays for three different solar array power outputs from about 20 kW to 300 kW. Cost savings are shown in the left column chart for the solar array wing prior to launch (blue columns) and placed in orbit (red columns), including launch cost. The two primary reasons for the concentrator cost savings are the much smaller cell area and cost, and the much lower mass, reducing launch costs. The primary reason for the mass savings is the inherently lower combined mass of the lens, radiator, and cell shielding for the concentrator compared to just the cell shielding for the one-sun cells, as discussed above.

VI. References

1. Mark O'Neill *et al.*, "Recent Space PV Concentrator Advances: More Robust, Lighter, and Easier to Track," 42nd IEEE Photovoltaic Specialists Conference, 2015, New Orleans.
2. Mark O'Neill *et al.*, "Space Photovoltaic Concentrator Using Robust Fresnel Lenses, 4-Junction Cells, Graphene Radiators, and Articulating Receivers," 43rd IEEE Photovoltaic Specialists Conference, 2016, Portland.
3. Mark O'Neill *et al.*, "Line-Focus and Point-Focus Space Photovoltaic Concentrators Using Robust Fresnel Lenses, 4-Junction Cells, & Graphene Radiators," 44th IEEE Photovoltaic Specialists Conference, 2017, Washington.

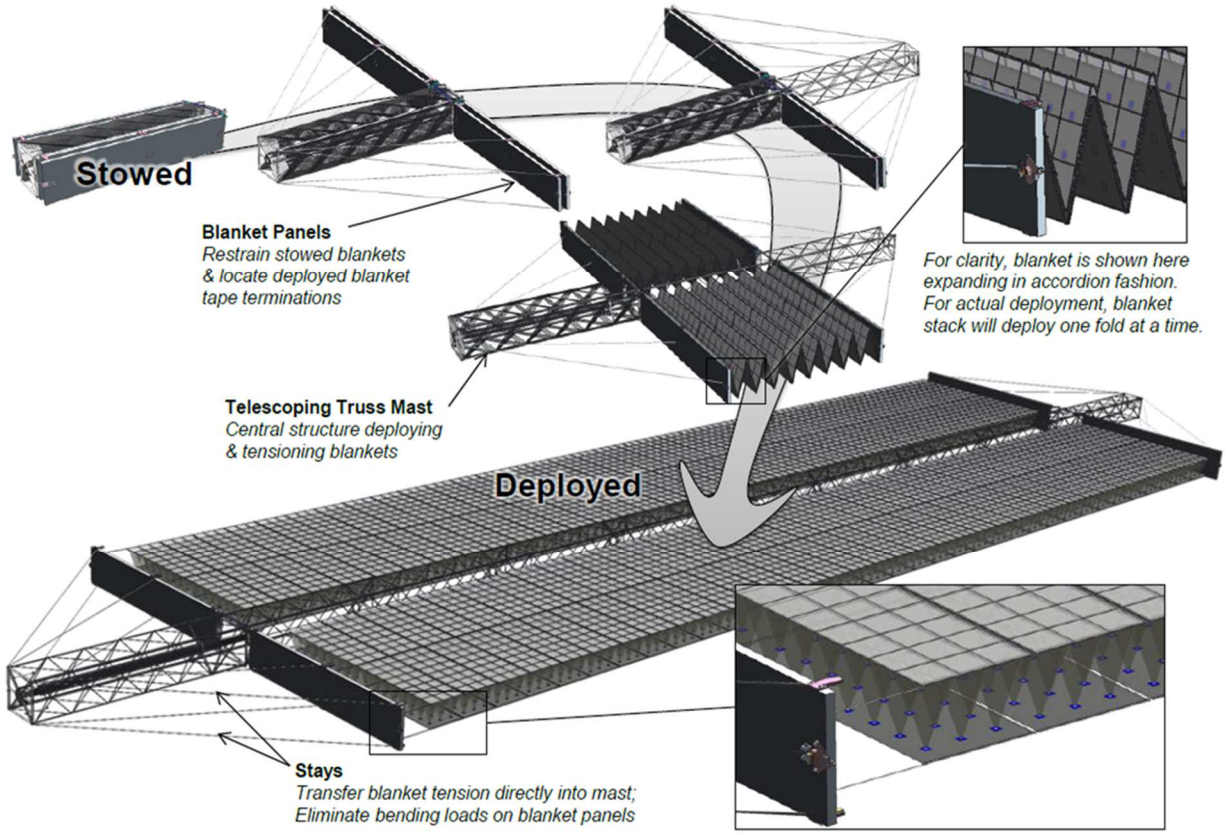

Fig. 14. 25X Point-Focus Concentrators on Compact Telescoping Array Platform for NASA's Extreme Environment Solar Power (EESP) Deep Space Missions [8].

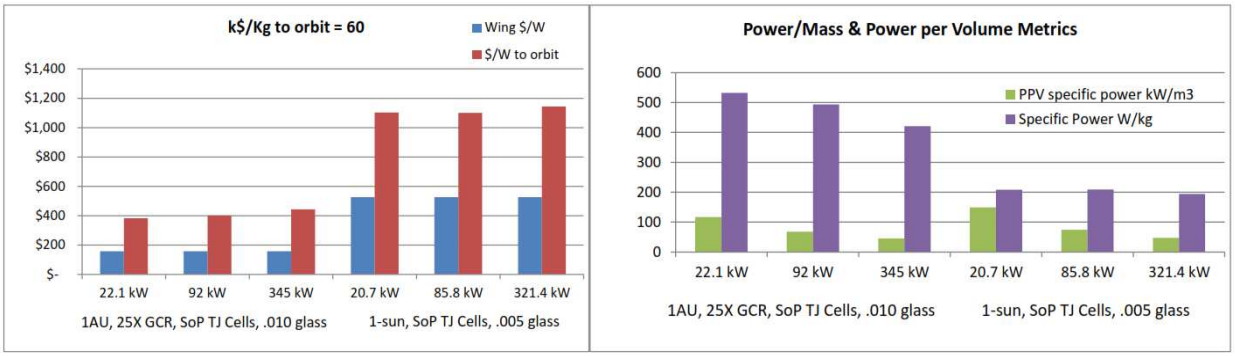

Fig. 15. Cost and Performance Metrics of Point-Focus Concentrators on Compact Telescoping Array [8].

4. Mark O'Neill *et al.*, "Advanced Development of Space Photovoltaic Concentrators Using Robust Lenses, Multi-Junction Cells, & Graphene Radiators," 7th World Conference on Photovoltaic Energy Conversion (WCPEC-7), 2018, Waikoloa.
5. Geoffrey Landis and James Fincannon, "Study of Power Options for Jupiter and Outer Planet Missions," 42nd IEEE Photovoltaic Specialists Conference, 2015, New Orleans.
6. Geoffrey Landis *et al.*, "Photovoltaic Power for Jupiter and Beyond," Space Photovoltaic Research & Technology 2016, Brook Park OH, Sept. 20-22, 2016.
7. Phillip Jenkins *et al.,* "TACSAT-4 Solar Cell Experiment: Two Years in Orbit, 10th European Space Power Conference (ESPC), Noordwijkerhout, the Netherlands, April 2014.
8. M. McEachen *et. al.*, "Point-Focus Concentration Compact Telescoping Array," Extreme Environments Solar Power Base Phase Final Report, Orbital ATK, Dec. 2017, NASA/CR-2017-219712.